

Numerically determined transport laws for fingering (“thermohaline”) convection in astrophysics

A. Traxler¹ and P. Garaud^{1,2}

¹ *Department of Applied Mathematics and Statistics, Baskin School of Engineering, UC Santa Cruz, 1156 High Street, Santa Cruz CA 95064*

² *On sabbatical leave at: Institute for Astronomy, 34 ‘Ohi‘a Ku St., Pukalani, HI 96768-8288*

S. Stellmach³

³ *Institut für Geophysik, Westfälische Wilhelms-Universität Münster, D-48149 Münster, Germany*

ABSTRACT

We present the first three-dimensional simulations of fingering convection performed in a parameter regime close to the one relevant for astrophysics, and reveal the existence of simple asymptotic scaling laws for turbulent heat and compositional transport. These laws can straightforwardly be extrapolated to the true astrophysical regime. Our investigation also indicates that thermocompositional “staircases,” a key consequence of fingering convection in the ocean, cannot form spontaneously in the fingering regime in stellar interiors. Our proposed empirically-determined transport laws thus provide simple prescriptions for mixing by fingering convection in a variety of astrophysical situations, and should, from here on, be used preferentially over older and less accurate parameterizations. They also establish that fingering convection does not provide sufficient extra mixing to explain observed chemical abundances in RGB stars.

Subject headings: hydrodynamics — instabilities — turbulence

1. Introduction

Recent years have seen rapidly growing interest in astrophysical applications of fingering convection (often referred to as “thermohaline convection”), a process by which the unequal diffusion rates of thermal and compositional fields can drive a double-diffusive instability and lead to significant turbulent transport across stably-stratified regions. In the Earth’s

oceans this process has been well-studied as “salt fingering” (see Stern 1960, or a recent review in Kunze 2003). In stellar contexts, by contrast, its exact form and contribution to vertical mixing is much less clear. Nevertheless, fingering convection has been invoked in various scenarios. It is thought to explain the lack of observed metallicity signatures from the infall of planets onto their host star (Vauclair 2004; Garaud 2010). It may also explain the presence of extra mixing in the radiative zones of RGB stars needed to fit abundance observations (Charbonnel & Zahn 2007; Stancliffe 2010; Denissenkov 2010).

While field, laboratory, and numerical measurements abound for salt fingering, data is much more scarce for the astrophysical regime. Transport by fingering convection in astrophysics has until now been modeled through mixing-length theory, commonly used parameterizations being those of Ulrich (1972) and Kippenhahn et al. (1980). In these works, turbulent compositional transport depends sensitively on the finger aspect ratio. As recently shown by Denissenkov (2010), however, there is a fundamental contradiction between the large aspect ratio required to explain abundance observations of RGB stars using these prescriptions (Charbonnel & Zahn 2007), and the near-unit aspect ratio of the “fingers” actually measured in his own two-dimensional simulations.

Three possibilities emerge to resolve this problem. First, the Kippenhahn et al. (1980) and Ulrich (1972) parameterizations may not adequately model transport by fingering convection. Secondly, two-dimensional simulations may not correctly capture the true dynamics of this inherently three-dimensional system. Finally, thermocompositional layers may form in the astrophysical objects studied, in which case transport could be strongly enhanced above the level of homogeneous fingering convection. Indeed, “staircases” of convectively mixed layers separated by thin fingering interfaces are ubiquitous in the ocean. In their presence, vertical mixing increases by as much as an order of magnitude above the already-enhanced mixing due to fingering (Schmitt et al. 2005; Veronis 2007). Whether such staircases form in astrophysics has never been established.

In this Letter we consider all three possibilities and present the first three-dimensional simulations to address directly the question of thermal and compositional transport by fingering convection in astrophysics. Using a high-performance algorithm specifically designed for homogeneous fingering convection, we are able to run simulations at moderately low values of the Prandtl number ($\text{Pr} = \nu/\kappa_T$) and diffusivity ratio ($\tau = \kappa_\mu/\kappa_T$), where ν is viscosity, and κ_T and κ_μ are the thermal and compositional diffusivities respectively. We find, in Section 3.1, asymptotic scaling laws for transport which are applicable to the stellar parameter regime ($\text{Pr} \ll 1, \tau \ll 1$). These provide a parameter-free, empirically-motivated prescription for mixing by homogeneous fingering convection. The compositional turbulent diffusivity derived is, as expected (Stern et al. 2001) a few times larger than that obtained

by Denissenkov (2010) for the same parameters, but remains too small to account for RGB abundance observations.

Since the presence of thermocompositional staircases is known to increase transport in the ocean, we next address the question of whether such staircases are likely to form spontaneously in the astrophysical context, in Section 3.2. Applying a recently-validated theory for staircase formation (Radko 2003; Stellmach et al. 2010), we find that they are in fact not expected to appear in this case. We conclude in Section 4 that our small-scale flux laws can reliably be used to estimate heat and compositional transport for a variety of astrophysical fingering systems and concur with Denissenkov’s view that fingering convection is not sufficient to explain the required extra mixing in RGB stars.

2. Model description and numerical algorithm

The dynamics of double-diffusive systems depend on the fluid properties ($\nu, \kappa_T, \kappa_\mu$), as well as its local stratification, measured by $\nabla - \nabla_{\text{ad}}$ (where $\nabla = d \ln T / d \ln p$ and $\nabla_{\text{ad}} = (d \ln T / d \ln p)_{\text{ad}}$ is the adiabatic gradient) and ∇_μ (where $\nabla_\mu = d \ln \mu / d \ln p$). Here T is temperature, p is pressure, and μ is the mean molecular weight. The fingering instability occurs in thermally stably-stratified systems ($\nabla - \nabla_{\text{ad}} < 0$) destabilized by an adverse compositional gradient ($\nabla_\mu < 0$). In most regimes of interest the main governing parameter is the density ratio, defined in astrophysics as (Ulrich 1972):

$$R_0^* = \frac{\nabla - \nabla_{\text{ad}}}{\nabla_\mu}. \quad (1)$$

This linear instability is well understood, thanks to early work in the oceanic context (Stern 1960; Baines & Gill 1969), later extended in astrophysics by Ulrich (1972) and Schmitt (1983). A system is Ledoux-unstable when $R_0^* < 1$, and fingering-unstable when $R_0^* \in [1, 1/\tau]$. Unfortunately, as discussed in Section 1, the nonlinear saturation of this instability, or in other words its turbulent properties, remain poorly understood.

We approach the problem from a numerical point of view, and model a fingering-unstable region using a local Cartesian frame (x, y, z) with gravity $\mathbf{g} = -g\mathbf{e}_z$. We run our numerical experiments using a high-performance spectral code, which was recently used to model three-dimensional fingering convection at oceanic parameters (Traxler et al. 2010), as well as thermohaline staircase formation (Stellmach et al. 2010). As a consequence of its original purpose, our code uses the Boussinesq approximation, which relates the density perturbations $\tilde{\rho}$ to the temperature and compositional perturbations \tilde{T} and $\tilde{\mu}$ via

$$\frac{\tilde{\rho}}{\rho_0} = -\alpha\tilde{T} + \beta\tilde{\mu}, \quad (2)$$

where ρ_0 is a reference density, $\alpha = -\rho_0^{-1}\partial\rho/\partial T$, and $\beta = \rho_0^{-1}\partial\rho/\partial\mu$. Fingering convection is driven by constant large-scale temperature and compositional gradients T_{0z} and μ_{0z} . These approximations, which greatly simplify the governing equations, are nevertheless justified since fingers are typically much smaller than a pressure or density scale height, and velocities are small compared with the sound speed. As first shown by Ulrich (1972), results in the Boussinesq case can straightforwardly be extended to the astrophysical case by replacing the Boussinesq density ratio $R_0 = \alpha T_{0z}/\beta\mu_{0z}$ with the true density ratio R_0^* defined in equation (1).

We now describe the governing equations in more detail. We express the velocity, temperature, and composition fields as the linear background stratification plus perturbations,

$$T(x, y, z, t) = T_0(z) + \tilde{T}(x, y, z, t), \quad (3)$$

$$\mu(x, y, z, t) = \mu_0(z) + \tilde{\mu}(x, y, z, t), \quad (4)$$

$$\mathbf{u}(x, y, z, t) = \tilde{\mathbf{u}}(x, y, z, t), \quad (5)$$

where $T_0(z) = T_{0z}z$ and $\mu_0(z) = \mu_{0z}z$. We nondimensionalize the system noting that an appropriate length scale is provided by the anticipated finger width (Stern 1960), $[l] = d = (\kappa_T\nu/g\alpha T_{0z})^{1/4}$. We then scale time using d^2/κ_T , temperature with $T_{0z}d$, and composition with $(\alpha/\beta)T_{0z}d$. The nondimensional governing equations are:

$$\frac{1}{\text{Pr}} \left(\frac{\partial \tilde{\mathbf{u}}}{\partial t} + \tilde{\mathbf{u}} \cdot \nabla \tilde{\mathbf{u}} \right) = -\nabla \tilde{p} + (\tilde{T} - \tilde{\mu})\mathbf{e}_z + \nabla^2 \tilde{\mathbf{u}}, \quad (6)$$

$$\nabla \cdot \tilde{\mathbf{u}} = 0, \quad (7)$$

$$\frac{\partial \tilde{T}}{\partial t} + \tilde{w} + \tilde{\mathbf{u}} \cdot \nabla \tilde{T} = \nabla^2 \tilde{T}, \quad (8)$$

$$\frac{\partial \tilde{\mu}}{\partial t} + \frac{1}{R_0} \tilde{w} + \tilde{\mathbf{u}} \cdot \nabla \tilde{\mu} = \tau \nabla^2 \tilde{\mu}, \quad (9)$$

Note that the Rayleigh number Ra then depends only on the computational domain height L_z :

$$\text{Ra} = \frac{\alpha g T_{0z} L_z^4}{\kappa_T \nu} = \left(\frac{L_z}{d} \right)^4. \quad (10)$$

We solve (6–9) in a triply-periodic box of size (L_x, L_y, L_z) , so that

$$\tilde{T}(x, y, z, t) = \tilde{T}(x + L_x, y, z, t) = \tilde{T}(x, y + L_y, z, t) = \tilde{T}(x, y, z + L_z, t), \quad (11)$$

and similarly for \tilde{p} , $\tilde{\mu}$ and $\tilde{\mathbf{u}}$.¹

¹Because the length scale of the convective motions is set by the diffusive scales in the fingering problem, it does not suffer from the known pathology of triply-periodic thermal convection, *i.e.* the homogeneous Rayleigh-Bénard problem (Calzavarini et al. 2006).

3. Results

3.1. Small-scale fluxes

Six sets of simulations were conducted at successively lower values of Pr and τ , for a range of density ratio values listed in Table 1 spanning in each case the instability range $R_0 \in [1, 1/\tau]$. As shown by Traxler et al. (2010), the statistical properties of fingering convection are independent of the computational domain size (i.e. of Ra and aspect ratio) provided it is wide enough to contain a sufficient number of fingers. The domain must also be tall enough to ensure that individual fingers do not span the entire height of the box. In most cases, the simulation domains were $67d \times 67d \times 107.2d$ with a resolution of 96^3 grid points. At the selected parameter values, this corresponds to approximately $5 \times 5 \times 10$ wavelengths of the fastest-growing mode (see Schmitt 1979), thus allowing space for many fingers to fit in the domain. As $R_0 \rightarrow 1/\tau$, where fingers tend to become more vertically elongated, wider and taller simulation domains ($83.75d \times 83.75d \times 268d$) were used to ensure that fingers remained uncorrelated across the box height. In sets 5 and 6 (the two lowest-diffusivity runs), lower finger heights allowed for shorter computational boxes ($67d \times 67d \times 67d$) but a higher resolution (192^3 grid points) was used to resolve the finer-scale structures. Near $R_0 = 1$, where the system dynamics are most turbulent, one additional simulation with twice the vertical resolution (192 or 384 points vertically) was run for each set. In all cases, the measured fluxes in the more fully-resolved run differed by no more than a few percent from the lower-resolution run, confirming that the spatial resolution used was sufficient to extract accurate fluxes. Sample snapshots of two of our simulations are shown in Figure 1. As an important note, we also find that, except when $R_0 \rightarrow 1/\tau$, the finger aspect ratio is close to unity (Denissenkov 2010).

We define non-dimensional heat and compositional fluxes through the Nusselt numbers Nu_T and Nu_μ , ratios of the total flux to the diffusive flux of the field considered. Equivalently, $\text{Nu}_{T,\mu} - 1$ represents the ratio of the turbulent diffusivity to the microscopic diffusivity. We measure Nu_T and Nu_μ from each simulation once the system has settled into a statistically-steady state. The results are summarized in Figure 2.

For ease of comparison between different simulation sets, we defined the rescaled density ratio as $r = (R_0 - 1)/(\tau^{-1} - 1)$ so that the instability range is $r \in [0, 1]$ in all cases. We find that *all simulation sets collapse onto a single universal profile* for the turbulent fluxes $\text{Nu}_T(r) - 1$ and $\text{Nu}_\mu(r) - 1$ as Pr and τ decrease, profiles which can be expressed as

$$\text{Nu}_T(r) - 1 = \tau^{3/2} \sqrt{\text{Pr}} f(r), \quad (12)$$

$$\text{Nu}_\mu(r) - 1 = \sqrt{\frac{\text{Pr}}{\tau}} g(r), \quad (13)$$

where the universal functions $f(r)$ and $g(r)$ are adequately fitted to the data using

$$g(r), f(r) \sim ae^{-br}(1-r)^c. \quad (14)$$

For $f(r)$ the data suggests that $a = 264$, $b = 4.7$, $c = 1.1$, and for $g(r)$ we find $a = 101$, $b = 3.6$, $c = 1.1$. Figure 2 shows these fits together with the rescaled Nusselt numbers. The physical interpretation of these scalings with τ and Pr is the following: for $\nu, \kappa_\mu \ll \kappa_T$, the instability is driven by the compositional field and the dependence of compositional transport on κ_T must drop out. The turbulent compositional diffusivity $D_\mu = (\text{Nu}_\mu - 1)\kappa_\mu$ is then proportional to the geometric mean of ν and κ_μ . The scaling for the temperature Nusselt number then follows by assuming that the nondimensional turbulent flux ratio $\gamma = \langle \tilde{w}\tilde{T} \rangle / \langle \tilde{w}\tilde{\mu} \rangle$ is always $O(1)$ (Radko 2003).

Although these simulations were conducted at parameter values a few orders of magnitude higher than those appropriate for stellar interiors, we find that they follow universal asymptotic laws. The simplicity of the system considered (e.g. no boundaries) also suggests that these laws *can* reliably be extrapolated to the astrophysical regime (as long as Pr is of order τ). From this we draw two critical observations. As found by Denissenkov (2010), the contribution of fingering convection to heat transport at stellar parameter values ($\text{Pr} \sim 10^{-6}$, $\tau \sim 10^{-6}$) is entirely negligible. It therefore does not affect the thermal structure of the object in any way. Compositional transport, on the other hand, can be significantly enhanced above molecular diffusion, by about two orders of magnitude depending on the ratio $\text{Pr}/\tau = \nu/\kappa_\mu$.

We now compare our flux laws with the parameterization of Ulrich (1972) and Kippenhahn et al. (1980), in which $\text{Nu}_\mu - 1 = C_p(L/W)^2/\tau R_0^*$, where L/W is the aspect ratio of the fingers (length L divided by width W) and C_p is a model constant ($C_p = 1$ for Kippenhahn et al. 1980, $C_p = 8\pi^2/3 \approx 26$ for Ulrich 1972). Figure 3 compares D_μ as a function of density ratio, at the fluid parameters used by Denissenkov (2010), $\text{Pr} = 4 \times 10^{-6}$ and $\tau = 2 \times 10^{-6}$. Given that the numerically-determined finger aspect ratio is close to one for all simulations as $\tau \ll 1$, $\text{Pr} \ll 1$, we find that the Ulrich (1972) prescription fares comparatively better than Kippenhahn et al. (1980). However, it still vastly overestimates mixing both near $R_0 = 1$ (where the system is closest to Ledoux instability) and $R_0 = 1/\tau$, close to linear stability. Crucially, our results show that the diffusivity obtained is not sufficient to explain RGB abundance observations for which a value of $C_p(L/W)^2 \approx 1000$ is needed (Charbonnel & Zahn 2007; Denissenkov 2010).

3.2. Layer formation

The small-scale flux laws presented above are accurate measurements of transport by *homogeneous* fingering convection. However, they may not appropriately describe transport in the presence of the kind of large-scale thermocompositional staircases which are known to form in oceanic thermohaline convection (*e.g.* Schmitt et al. 2005). The origin of such staircases has recently been discovered by Radko (2003), who demonstrated the existence of a positive feedback mechanism that can, in some circumstances, drive the growth of horizontally-invariant perturbations in the temperature and salinity fields: large-scale variations of the density ratio lead to convergences and divergences of fingering fluxes that reinforce the original perturbation, producing a growing disturbance that ultimately overturns into regular “steps.” This mechanism relies fundamentally on the variation of the flux ratio $\gamma = F_T/F_S$ (where F_T is the turbulent heat flux and F_S is the turbulent salt flux) with density ratio, and was therefore called the γ -instability. The γ -instability mechanism accurately predicts the growth rate of large-scale perturbations, and subsequent overturning into layers, in both two-dimensional simulations (Radko 2003), and three-dimensional simulations of staircase formation (Traxler et al. 2010; Stellmach et al. 2010). The instability requires that γ decreases as R_0 increases, a condition which must be experimentally determined from the fluxes for each set of fluid parameters Pr and τ .

In Radko’s original formulation for oceanic staircases, the systems of interest were dominated by turbulent fluxes. Diffusive contributions to the total fluxes were neglected for convenience and simplicity. However, as shown in Section 3.1, turbulent heat transport is negligible in the astrophysical case, so the γ -instability theory is re-derived here including all diffusive terms for accuracy and completeness. We begin with the equations of Section 2 and average them over many fingers:

$$\frac{1}{\text{Pr}} \left(\frac{\partial \mathbf{u}}{\partial t} + \mathbf{u} \cdot \nabla \mathbf{u} \right) = -\nabla p + (T - \mu) \mathbf{e}_z + \nabla^2 \mathbf{u} - \frac{1}{\text{Pr}} \nabla \cdot \mathbf{R}, \quad (15)$$

$$\frac{\partial T}{\partial t} + w + \mathbf{u} \cdot \nabla T = \nabla^2 T - \nabla \cdot \mathbf{F}_T, \quad (16)$$

$$\frac{\partial \mu}{\partial t} + \frac{1}{R_0} w + \mathbf{u} \cdot \nabla \mu = \tau \nabla^2 \mu - \nabla \cdot \mathbf{F}_\mu, \quad (17)$$

where \mathbf{u} , T , and μ now represent averaged large-scale fields. On the right-hand sides appear the usual Reynolds stress term, $R_{ij} = \overline{\tilde{\mathbf{u}}_i \tilde{\mathbf{u}}_j}$, and the turbulent fluxes $\mathbf{F}_T = \overline{\tilde{\mathbf{u}} \tilde{T}}$, $\mathbf{F}_\mu = \overline{\tilde{\mathbf{u}} \tilde{\mu}}$.

We proceed as in earlier formulations (Radko 2003; Traxler et al. 2010) by making several simplifying assumptions, the first being that Reynolds stresses are small enough to neglect and the second being that the turbulent fluxes are dominated by their vertical component, so that $\mathbf{F}_T \approx F_T \mathbf{e}_z$, $\mathbf{F}_\mu \approx F_\mu \mathbf{e}_z$. The γ -instability involves only the temperature

and compositional fields, so we consider only zero-velocity perturbations and discard the momentum equation. We then define the total fluxes as well as their ratio:

$$F_T^{\text{tot}} = F_T - (1 + \partial T/\partial z), \quad (18)$$

$$F_\mu^{\text{tot}} = F_\mu - \tau (1/R_0 + \partial\mu/\partial z), \quad (19)$$

$$\gamma^{\text{tot}} = \frac{F_T^{\text{tot}}}{F_\mu^{\text{tot}}}. \quad (20)$$

so that the thermal and compositional Nusselt numbers are:

$$\text{Nu}_T = \frac{F_T^{\text{tot}}}{-(1 + \partial T/\partial z)}, \quad \text{Nu}_\mu = \frac{F_\mu^{\text{tot}}}{-\tau(R_0^{-1} + \partial\mu/\partial z)}.$$

The final assumption is that Nu_T , Nu_μ , and γ^{tot} depend only on the local value of the density ratio R_ρ . Note that $R_\rho \neq R_0$ and may vary with z . We now linearize equations (16) and (17) around a state of homogeneous turbulent convection in which $T = 0 + T'$, $\mu = 0 + \mu'$, and $R_\rho = R_0 + R'$. For example, linearizing the density ratio R_ρ , we have:

$$\begin{aligned} R_\rho &= \frac{\alpha T_{0z}(1 + \partial T'/\partial z)}{\beta \mu_{0z}[1 + (\frac{\alpha T_{0z}}{\beta \mu_{0z}})\partial\mu'/\partial z]}, \\ &\approx R_0(1 + \partial T'/\partial z - R_0\partial\mu'/\partial z). \end{aligned} \quad (21)$$

The temperature equation yields

$$\begin{aligned} \frac{\partial T'}{\partial t} &= -\frac{\partial F_T^{\text{tot}}}{\partial z}, \\ &= \frac{\partial \text{Nu}_T}{\partial z} + \text{Nu}_T \frac{\partial^2 T'}{\partial z^2}, \\ &= \frac{\partial \text{Nu}_T}{\partial R_\rho} \Big|_{R_0} \frac{\partial R_\rho}{\partial z} + \text{Nu}_T(R_0) \frac{\partial^2 T'}{\partial z^2}, \\ &= \frac{\partial \text{Nu}_T}{\partial R_\rho} \Big|_{R_0} R_0 \left(\frac{\partial^2 T'}{\partial z^2} - R_0 \frac{\partial^2 \mu'}{\partial z^2} \right) + \text{Nu}_T(R_0) \frac{\partial^2 T'}{\partial z^2}. \end{aligned} \quad (22)$$

and similarly for equation (17). Assuming normal modes of the form $T', \mu' \sim e^{ikz + \lambda t}$, equations (22) and the equivalent linearization of (17) combine into the quadratic

$$\lambda^2 + \lambda k^2 \left[\text{Nu}_0(1 - A_1 R_0) + A_2 \left(1 - \frac{R_0}{\gamma_0^{\text{tot}}} \right) \right] - k^4 A_1 \text{Nu}_0^2 R_0 = 0, \quad (23)$$

where we use the following notation for simplicity:

$$\begin{aligned} A_1 &= R_0 \frac{d(1/\gamma^{\text{tot}})}{dR_\rho} \Big|_{R_0}, \quad A_2 = R_0 \frac{d\text{Nu}_T}{dR_\rho} \Big|_{R_0}, \\ \text{Nu}_0 &= \text{Nu}_T(R_0), \quad \gamma_0^{\text{tot}} = \gamma^{\text{tot}}(R_0). \end{aligned}$$

Note that this is identical to the quadratic of Radko (2003) replacing γ by γ^{tot} .

As discussed by Radko (2003), a sufficient condition for the instability is that γ^{tot} is a decreasing function of density ratio. Indeed, when this is the case, the coefficient A_1 is positive, and the expression (23) has two real roots, one positive and one negative. In order to determine whether the γ -instability occurs and therefore whether staircases may spontaneously form at low Pr, low τ , we simply need to calculate γ^{tot} from our previous measurements. The results are shown in Figure 4. We find that the flux ratio always increases with density ratio. Crucially, this suggests that thermocompositional layers are not expected to form spontaneously in astrophysical fingering convection. In the absence of such “staircases,” the fluxes are accurately supplied by our flux laws 12 and 13.

4. Conclusion

Our results can be summarized in a few key points. Using high-performance three-dimensional numerical simulations we find that turbulent compositional transport by fingering convection follows the simple law:

$$D_\mu = \kappa_\mu(\text{Nu}_\mu - 1) = 101\sqrt{\kappa_\mu\nu}e^{-3.6r}(1-r)^{1.1}, \quad (24)$$

where $r = (R_0^* - 1)/(\tau^{-1} - 1)$. Meanwhile, the turbulent heat flux is negligibly small at stellar parameters (see Denissenkov 2010). We also find that large-scale thermocompositional staircases are not expected to form spontaneously for Pr, $\tau \ll 1$, so that the turbulent diffusivity proposed above may and should be used as given to model astrophysical fingering convection.

Applying these findings to the problem of RGB stars, we concur with Denissenkov’s conclusion that mixing by fingering convection alone cannot explain the observed RGB abundances, and that additional mechanisms should be investigated instead (*e.g.* gyroscopic pumping, see Garaud & Bodenheimer 2010). A second example of application to the planetary pollution problem is presented in a companion paper (Garaud 2010).

A.T. and P.G. are supported by the National Science Foundation, NSF-0933759. S.S. was supported by grants from the NASA Solar and Heliospheric Program (NNG05GG69G, NNG06GD44G, NNX07A2749).

Figure 1 was rendered using VAPOR (Clyne et al. 2007; Clyne & Rast 2005), a product of the National Center for Atmospheric Research.

REFERENCES

- Baines, P., & Gill, A. 1969, *J. Fluid Mech.*, 37
- Calzavarini, E., Doering, C. R., Gibbon, J. D., Lohse, D., Tanabe, A., & Toschi, F. 2006, *Phys. Rev. E*, 73, 035301
- Charbonnel, C., & Zahn, J. 2007, *Astron. Astrophys.*, 467
- Clyne, J., Mininni, P., Norton, A., & Rast, M. 2007, *New J. Phys*, 9
- Clyne, J., & Rast, M. 2005, in *Proceedings of Visualization and Data Analysis 2005*
- Denissenkov, P. A. 2010, ArXiv e-prints
- Garaud, P. 2010, submitted to *ApJ Letters*
- Garaud, P., & Bodenheimer, P. 2010, *ApJ*, 719, 313
- Kippenhahn, R., Ruschenplatt, G., & Thomas, H. 1980, *A&A*, 91, 175
- Kunze, E. 2003, *Prog. Oceanogr.*, 56, 399
- Radko, T. 2003, *J. Fluid Mech.*, 497, 365
- Schmitt, R. 1979, *Deep-Sea Res.*, 26A, 23
- . 1983, *Phys. Fluids*, 26, 2373
- Schmitt, R., Ledwell, J., Montgomery, E., Polzin, K., & Toole, J. 2005, *Science*, 308, 685
- Stancliffe, R. J. 2010, *MNRAS*, 403, 505
- Stellmach, S., Traxler, A., Garaud, P., Brummell, N., & Radko, T. 2010, ArXiv e-prints
- Stern, M. 1960, *Tellus*, 12, 172
- Stern, M., Radko, T., & Simeonov, J. 2001, *J. Mar. Res.*, 59, 355
- Traxler, A., Stellmach, S., Garaud, P., Radko, T., & Brummell, N. 2010, ArXiv e-prints
- Ulrich, R. K. 1972, *ApJ*, 172, 165
- Vauclair, S. 2004, *Astrophys. J.*, 605, 874
- Veronis, G. 2007, *Deep-Sea Res. I*, 54

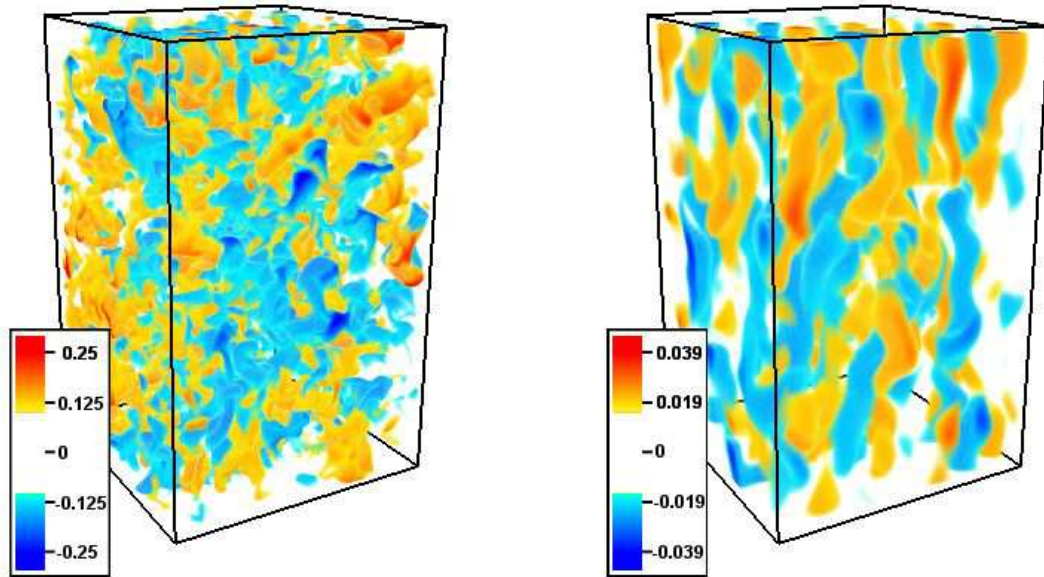


Fig. 1.— Compositional perturbations, in units of the compositional contrast across the height of the domain, of two simulations at $\text{Pr} = \tau = 1/10$, at density ratio $R_0 = 1.45$ (left) and $R_0 = 9.1$ (right). In general, fingering convection is more laminar, and the fingers are taller as $R_0 \rightarrow 1/\tau$ (as the background stratification becomes more stable). However, as Pr and τ decrease, secondary instabilities enforce shorter fingers even at high density ratio.

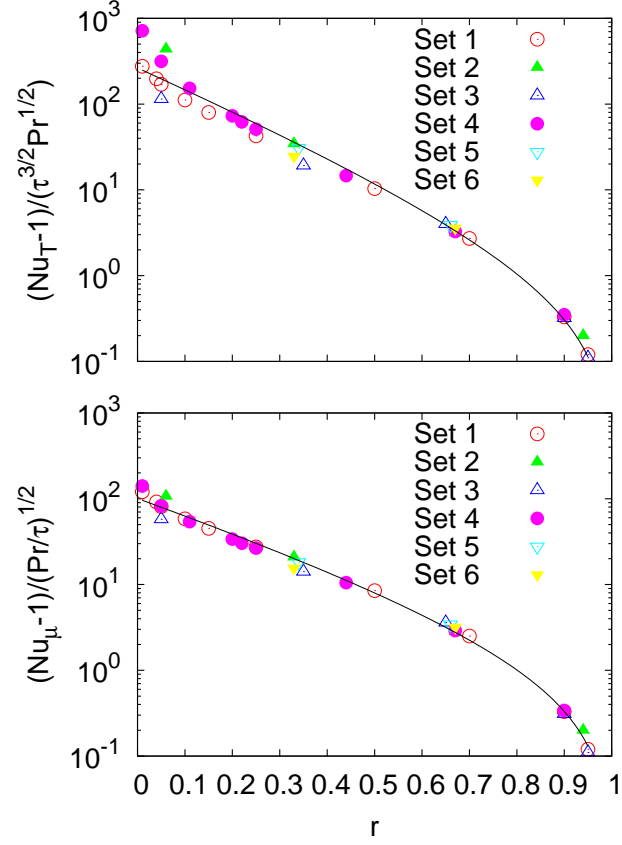


Fig. 2.— Turbulent heat and compositional fluxes as a function of rescaled density ratio r . Dividing the turbulent heat flux by $\tau^{3/2}Pr^{1/2}$ and compositional flux by $\sqrt{Pr/\tau}$ reveals the universal scaling laws (12) and (13). Also shown are $f(r)$ and $g(r)$ fitted to the data (solid lines).

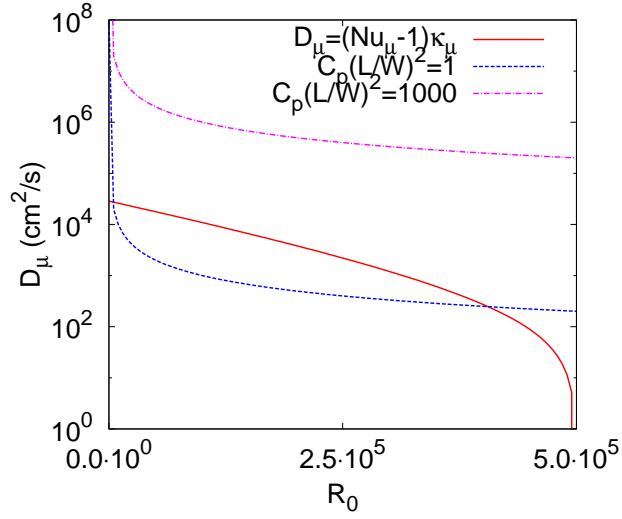


Fig. 3.— Comparison between our empirically-determined compositional turbulent diffusivity and the parameterizations of Kippenhahn et al. (1980) and Ulrich (1972) (where the coefficient $C_p(L/W)^2$ serves as a free parameter). Since we find $L/W \sim 1$, Kippenhahn et al. (1980) underestimates D_μ for most of the R_0 range and overestimates it as $R_0 \rightarrow 1$ and $R_0 \rightarrow 1/\tau$. Ulrich (1972) fares slightly better at intermediate R_0 . Our results show that turbulent mixing by fingering convection is not sufficient to explain observations, for which $C_p(L/W)^2 \sim 1000$ is required (see text for detail).

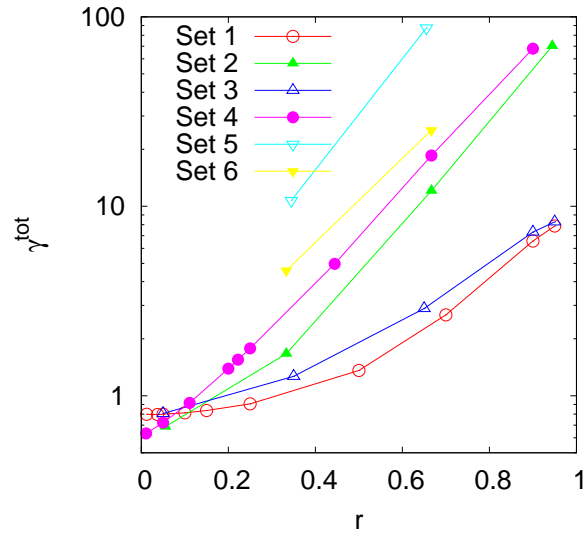


Fig. 4.— The total flux ratio $\gamma^{\text{tot}} = F_T^{\text{tot}}/F_\mu^{\text{tot}}$ for various systems. As the density stratification becomes more stable ($r \rightarrow 1$), the fluxes of heat and composition are dominated by diffusive contributions and their ratio approaches the limiting value R_0/τ . The flux ratio increases monotonically with r , indicating that staircases will not form spontaneously in this parameter regime ($\text{Pr} \ll 1, \tau \ll 1$).

Table 1: Summary of governing parameters for all simulation sets.

Set	Pr	τ	R_0
1	1/3	1/3	1.025, 1.075, 1.1, 1.1 ^{α} , 1.1 ^{β} , 1.125, 1.2, 1.3, 1.5, 2, 2.4, 2.8, 2.9 ^{a,α}
2	1/3	1/10	1.5, 1.5 ^{β} , 4, 7, 9.5 ^{a,α}
3	1/10	1/3	1.1, 1.1 ^{α} , 1.7, 2.3, 2.8 ^{a,α} , 2.9 ^{a,α}
4	1/10	1/10	1.1, 1.45, 1.45 ^{α} , 2, 2.8, 3, 3.3, 5, 7, 9.1 ^{a,α}
5	1/10	1/30	11 ^{b,γ} , 11 ^{b,δ} , 20 ^{b,γ}
6	1/30	1/10	4 ^{b,γ} , 7 ^{b,γ}

Note. — Relevant parameters include values of Pr and τ , of the density ratio $R_0 \in [1, 1/\tau]$, domain size, and resolution. Unless otherwise specified (see footnotes), simulations were run at domain sizes of $67 \times 67 \times 107.2d$ and resolution of 96^3 grid points.

^{a} $83.75d \times 83.75d \times 268d$

^{b} $67d \times 67d \times 67d$

^{α} $96 \times 96 \times 192$

^{β} $192 \times 192 \times 384$

^{γ} $192 \times 192 \times 192$

^{δ} $384 \times 384 \times 384$